Threshold Dynamics of Singular Gravity-Capillary Waves

Christopher L. Goodridge, W. Tao Shi, and Daniel P. Lathrop*
Department of Physics, Emory University, Atlanta, Georgia 30322
(Received 1 September 1995)

Surface wave experiments confirm predictions of a threshold amplitude for droplet ejection. Droplet ejection and spray originate from highly focused surface singularities in the simplest states. The threshold is found to be dependent on forcing frequency and surface tension in accordance with a simple scaling theory presented here. Linear stability analysis indicates that the dynamics of the ejections at low frequency are low dimensional. Observations confirm this, and show periodic ejections as the simplest observed state. Ejecting states at higher frequency appear turbulent in nature.

PACS numbers: 47.20.Ma, 47.55.Dz, 68.10.–m, 92.10.Hm

The droplets, spray, and foam, produced by waves breaking on a beach [1] and breaking deep water waves [2], are examples of dynamical singularities on the free surface of a liquid. This work details observations of free surface wave singularities which give rise to droplet ejection. Dynamical singularities, local time dependent amplitude or gradient divergences, play an important role in the behavior of a number of other physical systems such as turbulent dissipation fluctuations [3], self-focusing in nonlinear optical systems [4], cavitation phenomena and sonoluminescence [5], and gravitational singularities [6]. Significant mysteries exist about what classes of motion and what types of singularities arise in spatially extended systems.

Induced surface waves allow close observation of singularity formation in a familiar nonlinear system. Here surface wave singularities were produced on a liquid surface by vertically oscillating a container. The flat surface becomes unstable to periodic surface waves at a critical acceleration (via the Faraday instability [7]). As the excitation is increased further, we observe a sharp transition to a state with spikes on the surface which eject droplets from the tip. Much is already known about the onset of periodic surface waves and the existence of spatial and temporal chaos in this system [7–11]. Recent theoretical and experimental studies of free surfaces have shown root-type singularities in droplet breakoff [12]. In that case, the gradient of the surface diverges while the height remains bounded. We conjecture that we have observed a type of strong singularity on a free surface where the height of the surface diverges in the zero surface tension limit. This phenomenon is closely related to the theoretical predictions, of Newell and Zakharov [13], of a transition from a simply connected surface to a multiply connected surface with droplet ejection and air entrainment.

We have observed droplet ejection over a large frequency range in a variety of fluids (water, ethanol, and water/glycerin solutions [14]). The threshold for ejection singularities depends strongly on the forcing frequency. The threshold also depends on the surface tension of the liquid, but only weakly on other fluid parameters or container geometry. Droplet ejection was observed in both gravity waves and capillary waves. Gravity and capillary waves are defined from the dispersion relation for infinite depth periodic waves [15]

$$\omega^2 = gk + (\sigma/\rho)k^3, \tag{1}$$

where ω is the angular frequency, k the wave number, σ the surface tension, ρ the density, and g the acceleration due to gravity. The crossover wave number, $k_0 = \sqrt{g\rho/\sigma}$, and the corresponding frequency, $\omega_0 = (4g^3\rho/\sigma)^{1/4}$, define low frequency gravity ($\omega < \omega_0$) and high frequency capillary ($\omega > \omega_0$) wave ranges. Low frequency (gravity) waves still experience capillary effects due to the length scale of the droplet ejecting peaks.

Two examples of droplet ejecting states can be seen in Fig. 1. The first photograph [Fig. 1(a)] is an example of an excited gravity wave showing an ejection spike. It is notable that although the excitation occurs in gravity length scales the fluid motion transfers energy to capillary length scales in the spike. Figure 1(b) is in the frequency domain where capillary waves are directly excited to eject [16].

We have analyzed the motion of the ejections for low frequency gravity states by employing video imaging and high speed movies. The wave motion is characterized by a slow growth of the wave peak amplitude over a number of wave periods. The ejection is preceded, by one period, by a rounded wave peak whose amplitude increases until the slope becomes infinite and a slight overhang is formed. This last smooth wave collapses into a sharp-cornered depression, which then focuses to form a growing spike. The spike increases in amplitude and width and suffers droplet producing Rayleigh instabilities [17] near the cylindrical top. Finally, it collapses due to gravitational forces, leaving behind a stretched neck which also breaks into droplets [12]. The collapsing spike often entrains bubbles into the fluid bulk.

Image analysis applied to Fig. 1 and other images indicates that the surface height in the body of the ejection fit a power law

$$h(r) \sim 1/r^{\alpha}, \tag{2}$$

 0031-9007/96/76(11)/1824(4)$10.00

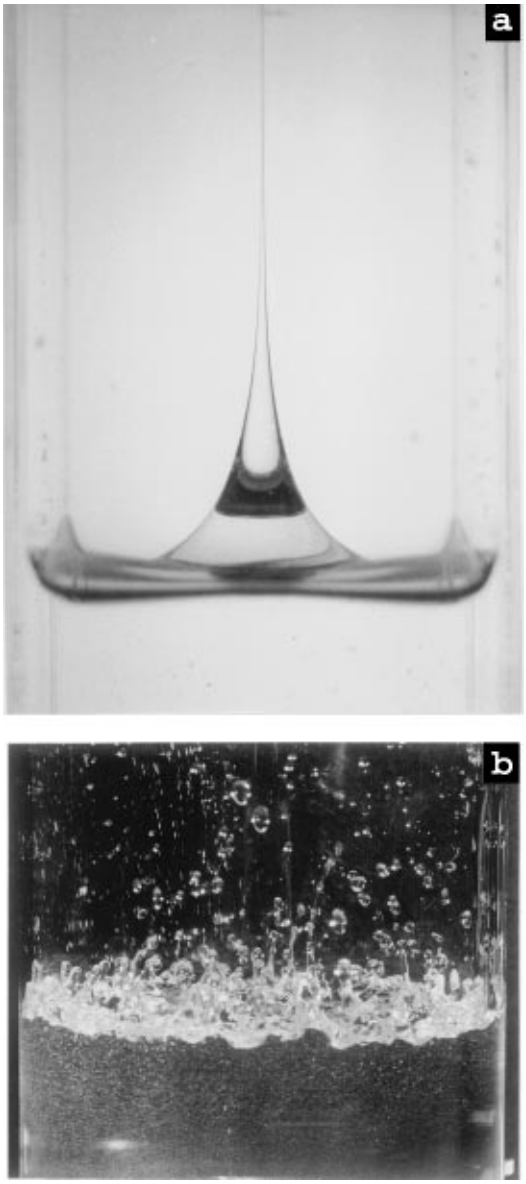

FIG. 1. (a) An ejecting state in the gravity regime experiencing excitation at frequency 7.1 Hz and peak acceleration of 426 cm/s^2 is shown in a glycerin-water solution (viscosity $\nu \sim 310$ cm/s^2). (b) Ejections occur in a turbulent capillary wave state at 30 Hz in water. Note air bubbles dispersed below the surface.

where $\alpha = 0.53 \pm 0.13$. The cylindrical coordinates h and r are, respectively, the height and the radius of the fluid column in a cylindrical coordinate system defined around the spike axis. This supports the hypothesis that these ejections are a type of strong singularity. The $h(r)$ relation above with $\alpha = 0.5$ is consistent with a solution to the Bernoulli equation and the free surface boundary condition which has the same power law form (to be presented in a later paper). Large scale cutoffs are set by the wavelength of the underlying waves; a small scale cutoff is imposed by capillary instabilities which produce droplets near the tip.

The low and high frequency ranges have different droplet ejecting behavior. Gravity wave states eject from positions consistent with the underlying periodic states; capillary wave states eject at random positions. The time dynamics for the gravity waves are relatively low dimensional while those for the capillary waves are turbulent.

In order to characterize the transition to ejecting waves, we have measured the threshold acceleration as a function of forcing frequency. An Unholtz-Dickie TA100-20 electrodynamic shaker supplied the excitation used to determine the threshold acceleration data shown in Fig. 2. A glass reaction flask with an inner diameter of 13.5 cm containing 1200 ml of fluid was mounted on the armature of the shaker. Two different fluids with different surface tensions were used: distilled water ($\sigma = 72$ dyn/cm) and ethyl alcohol ($\sigma = 23$ dyn/cm). Hysteresis exists in the ejection threshold in the gravity wave range [on the order of (5–10)%] while capillary wave states appear to be nonhysteretical. Long time transient states have been observed throughout the frequency range observed.

The threshold point was determined by supplying sufficient force to produce vigorous droplet ejection and then lowering the magnitude until the ejections terminated. The droplets were detected visually and sufficient time was allowed to elapse to be certain that all transient states had passed. The acceleration was determined using an Omega ACC103 accelerometer attached to the armature. Threshold acceleration measurements for distilled water in

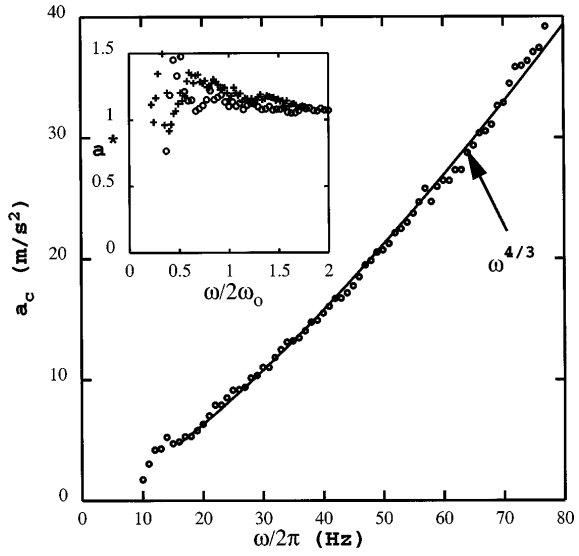

FIG. 2. The critical acceleration a_c for droplet ejection in water (in a circular container 13.5 cm in diameter) as a function of frequency shows an $a_c = 2.39\omega^{4/3}(\sigma/\rho)^{1/3}$ dependence for frequencies in the capillary range. At lower freqencies, the threshold function is more complicated due to a dependence on the low lying modes of the container. The inset shows the nondimensional threshold acceleration for both water (○) and ethanol (+) in order to test the surface tension dependence.

the frequency range of 10 to 80 Hz can be seen in Fig. 2. This range encompasses the crossover point from gravity to capillary waves for the fluids used (27.0 Hz for water, and 44.8 Hz for ethanol [18]).

The critical acceleration is dependent on the frequency of the vertical excitation and the surface tension of the fluid. There is only one dimensionally consistent form which combines these two parameters to yield an acceleration: $a_c \sim \omega^{4/3}(\sigma/\rho)^{1/3}$. This agrees well with the threshold measurements taken in water in the capillary wave range; a regression analysis indicates an $a_c \sim \omega^{1.34}$ dependence. Fitting this acceleration to the water data in the capillary range yields the prefactor and the expression becomes

$$a_c = 2.39\omega^{4/3}(\sigma/\rho)^{1/3}. \quad (3)$$

In order to test the surface tension scaling, we have nondimensionalized the water and ethanol data using capillary length and time scales. The nondimensionalized acceleration is [19]

$$a^* \equiv (2\pi)^2(\sigma/\rho)^{-1/3}\omega^{-4/3}a_c. \quad (4)$$

The frequency is nondimensionalized using the gravity-capillary crossover excitation frequency ($2\omega_0$). Although this removes most of the fluid parameter dependence, the imperfection of the data collapse may indicate an additional viscous dependence of the threshold. The effects of viscosity on droplet ejection will be discussed in detail in a forthcoming paper.

A better understanding of the dynamics of the ejecting state follows from the well-known linear stability analysis for this system [8]. The number of linearly unstable modes increases with frequency at threshold (Fig. 3). This is due both to the increased density of states for the linear modes (here Bessel modes) and to the increased width of the instability cones [10] for each mode (which causes the modes to increasingly overlap at higher accelerations). At lower frequencies only a few modes are excited.

This suggests relatively simple time dynamics are possible at low frequencies. In the simplest cases, as the amplitude of the forcing is increased the system exhibits the following states: a quiescent state with no waves, a periodic wave state at half the forcing frequency, and finally a state with periodic ejections.

In contrast to this simple scenario, the number of unstable modes increases rapidly as the frequency is increased. This is consistent with the observations that at low frequency the simplest dynamics of the ejections observed appear periodic, while at higher frequency the ejecting states appear turbulent. These higher frequency states have ejections with locations that appear random in time and space, whereas at low frequencies the locations are fixed by the modes of the container.

To determine the time dynamics of the states we have employed a global indicator—the vertical position of the tank. Although the forcing is sinusoidal, the reaction forces due to the fluid cause the small additional motions which reflect the wave state. The position was determined

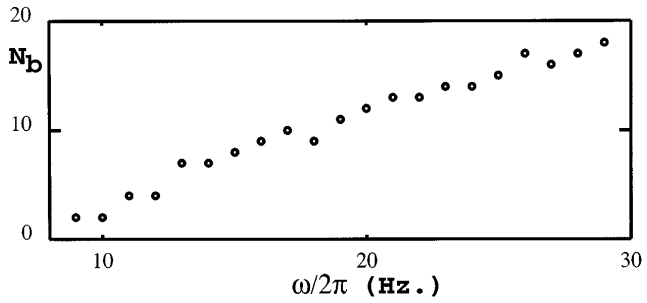

FIG. 3. The number of simultaneous excited Bessel modes at threshold (from linear stability analysis) in the circular container, 13.5 cm in diameter.

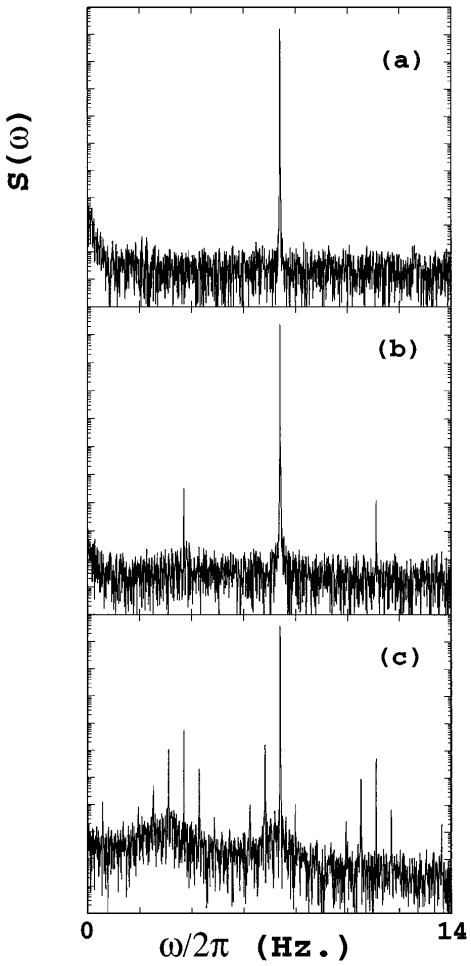

FIG. 4. Here the power spectrum of axial motion for a glycerin-water solution ($\nu \sim 250$ cm^2/s) illustrates wave states at different excitations: (a) At 296 cm^2/s^2 there is no wave motion (only the periodic 7.4 Hz motion is evident), (b) at 381 cm/s^2 the periodic waves at half the forcing frequency are evident also, and (c) at 494 cm/s^2 a periodic droplet ejecting state shows peaks at multiples of $\omega_0/12$. This state ejects every 12 forcing oscillations. States which eject every 14 forcing oscillations have also been observed.

using a Novotechnik T150 linear potentiometer with 1 μm resolution. The potentiometer was instrumented using a Wheatstone bridge driven by a lock-in amplifier at 10 kHz. The Fourier spectra for the time series of axial position for various accelerations can be seen in Fig. 4, including one where the ejections occur periodically (but the droplets and bubbles produced vary slightly in size and shape).

We have observed the predicted droplet ejections in vertically excited surface waves and determined a relationship between the threshold acceleration for droplet ejection and the fundamental fluid parameters and forcing frequency. As indicated by linear stability analysis, the ejecting states become more complicated as the driving frequency is increased. We have also observed the time dynamics of the system, including periodic ejecting states.

The authors would like to thank a number of people for helpful discussions and assistance in the preparation of this manuscript, including R. Behringer, M. P. Brenner, W. S. Edwards, C. Doering, H. G. E. Hentschel, D. Lohse, S. Perkowitz, H. L. Swinney, and B. Zeff. This work was partially supported by the Emory University Research Committee.

*Electronic address: dpl@complex.physics.emory.edu

[1] D. H. Peregrine, Annu. Rev. Fluid Mech. **15**, 149 (1983).
[2] M. L. Banner and D. H. Peregrine, Annu. Rev. Fluid Mech. **25**, 373 (1993).
[3] K. R. Sreenivasan and C. Meneveau, Phys. Rev. A **38**, 6287 (1988).
[4] Y. R. Shen, *The Principles of Nonlinear Optics* (John Wiley and Sons, Inc., New York, 1984).
[5] R. T. Knapp, J. W. Dailey, and F. G. Hammitt, *Cavitation* (McGraw-Hill Book Company, New York, 1970); D. F. Gaitan, L. A. Crum, C. C. Church, and R. A. Roy, J. Acoust. Soc. Am. **91**, 3166 (1992).
[6] S. W. Hawking and G. F. R. Ellis, *The Large Scale Structure of Space-Time* (Cambridge University Press, London, 1973).
[7] M. Faraday, Philos. Trans. R. Soc. London **121**, 299 (1831).
[8] T. B. Benjamin and F. Ursell, Proc. R. Soc. London Ser. A **225**, 505 (1954).
[9] S. Douady, J. Fluid Mech. **221**, 383 (1990); S. Cilberto, S. Douady, and S. Fauve, Europhys. Lett. **15**, 23 (1991).
[10] W. S. Edwards and S. Fauve, Phys. Rev. E **47**, R788 (1993).
[11] N. B. Tufillaro, R. Ramshankar, and J. P. Gollub, Phys. Rev. Lett. **62**, 422 (1989); J. Miles and D. Henderson, Annu. Rev. Fluid Mech. **22**, 143 (1990); O. N. Mesquita, S. Kane, and J. P. Gollub, Phys. Rev. A **45**, 3700 (1992).
[12] J. Eggers, Phys. Rev. Lett. **71**, 3458 (1993); M. P. Brenner, X. D. Shi, and S. R. Nagel, *ibid.* **73**, 3391 (1994).
[13] A. C. Newell and V. E. Zakharov, Phys. Rev. Lett. **69**, 1149 (1992).
[14] Contamination of the solutions was minimized by thoroughly cleaning the containers, using distilled water and reagent grade glycerin and alcohols, and sealing the containers.
[15] L. D. Landau and E. M. Lifshitz, *Fluid Mechanics* (Pergamon Press, New York, 1987).
[16] Figures 1(a) and 4 were produced in a square Plexiglas tank 11.6 cm on edge containing 527 ml of glycerin/water solution [92% glycerin 8% distilled water by volume for Fig. 1(a) and 91% glycerin 9% distilled water by volume for Fig. 4]. Figure 1(b) was excited in distilled water in a cylindrical tank 13.5 cm in diameter. An electromagnetic linear actuator supplied the sinsusoidal driving force and an air bearing was used to maintain strict vertical motion. The first photograph was taken using a strobe light triggered by the forcing oscillation; the second was taken by mounting a flash above and behind the tank.
[17] S. Chandrasekhar, *Hydrodynamic and Hydromagnetic Stability* (Dover Publications, Inc., New York, 1981).
[18] The simplest free surface response to vertical excitation is at one half the excitation frequency so the crossover excitation frequency is twice ω_0.
[19] This nondimensionalization is arrived at by taking a nondimensional acceleration $a^* = a(\rho/\sigma)l^2$ and using the corresponding wavelength $\lambda = l$ from the capillary dispersion relation.